Springer

Journal of Mechanical Science and Technology 23 (2009) 3088~3094

Journal of Mechanical Science and Technology

www.springerlink.com/content/1738-494x
DOI 10.1007/s12206-009-0818-1

A new planar 3-DOF parallel mechanism with continuous 360-degree rotational capability †

TaeWon Seo*, Woosung In and Jongwon Kim

School of Mechanical and Aerospace Engineering, Seoul National University, Seoul, Korea

(Manuscript received November 19, 2008; Revised July 20, 2009; Accepted August 3, 2009)

Abstract

This paper presents a novel three degrees of freedom (3-DOF) planar parallel mechanism with a 360-degree rotational capability, which can be used as a positioning device. A high rotational capability is necessary to reduce process time and to apply the mechanism to various fields such as micro-machining and printed circuit board (PCB) depaneling. The proposed mechanism has the advantage of a continuous rotational capability over existing planar parallel mechanisms with limited rotation. The position and velocity kinematics are derived, and the singularities are analyzed based on the Jacobian matrices. The workspace can be determined not to have a singularity inside, and the kinematic variables for enlarging the singularity-free workspace are determined. The application example on the PCB depaneling process is proposed for future work.

***Keywords*:** Kinematics; Planar parallel mechanism; Rotational capability; Three degrees of freedom

1. Introduction

A parallel mechanism is one with a closed loop of several serial chains. Parallel mechanisms have more chains and less moving inertia than serial mechanisms, which leads to them having comparative advantages of higher speeds, better stiffness, and improved positioning accuracies [1]. Due to these advantages, parallel mechanisms have received increasing attention from industries and universities in recent decades.

However, from an application point of view, the parallel mechanism has a major drawback in its limited rotational capability. The Stewart-Gough mechanism, which is a well-known standard of the 6-DOF parallel mechanism, can only realize 30 degrees of rotation [2]. To overcome this drawback, Kim et al. suggested the Eclipse-I and -II mechanisms to be applied in a 5-axis machine tool and motion simulator by realizing a 90-degree rotation and a 360-degree rotation, respectively [3, 4].

However, the Eclipse mechanisms are designed to be used in spatial motions, and thus they are inefficient when used exclusively in planar motions. The planar parallel mechanism has some comparative advantages over the stack-type serial mechanism with the *X-Y* stage motions, and the additional rotational axis results in error accumulation, moving inertia, and stiffness. Thus, several planar parallel mechanisms have also been proposed [5-11], but the rotational capability of these parallel mechanisms is limited. Therefore, the mechanisms are not suitable for some industrial applications such as micro-machining and PCB depaneling [12, 13], where a high rotational capability is necessary to reduce process time and to apply the mechanism to various tasks.

This paper presents a new planar 3-DOF mechanism capable of a continuous 360-degree rotation as well as *X-Y* translational motions. Figs. 1 and 2 illustrate the architecture and rotational capability of the mechanism, respectively. The proposed mechanism is

† This paper was recommended for publication in revised form by Associate Editor Dae-Eun Kim

*Corresponding author. Tel.: +82 2 880 7144, Fax.: +82 2 875 4848
E-mail address: taewon.seo1@gmail.com

motivated by the Eclipse mechanism, which has some advantages over the Eclipse-I mechanism. They are as follows.

- The mechanism can be designed not to have singularity configurations in the workspace, so it does not need over-actuation.
- The number of actuators can be reduced from eight to three to realize the planar motion.
- The stiffness can be enhanced by removing the spherical joint.
- The mechanism is more suitable for the design of a combined machine with serial mechanisms.

The proposed planar mechanism consists of 3-PPR (where P and R denote prismatic and revolute joints, respectively) serial sub-chains. As the first P denotes the actuated P moving along the fixed circular guide, continuous rotational motion can be realized. The three arrows in Fig. 1 denote the actuated circular Ps. Kinematics, Jacobian, singularity, and workspace analyses are discussed based on the mechanism. A practical application example of PCB depaneling system is presented next.

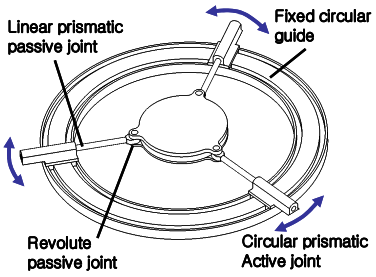

Fig. 1. Architecture of the novel 3-DOF planar mechanism.

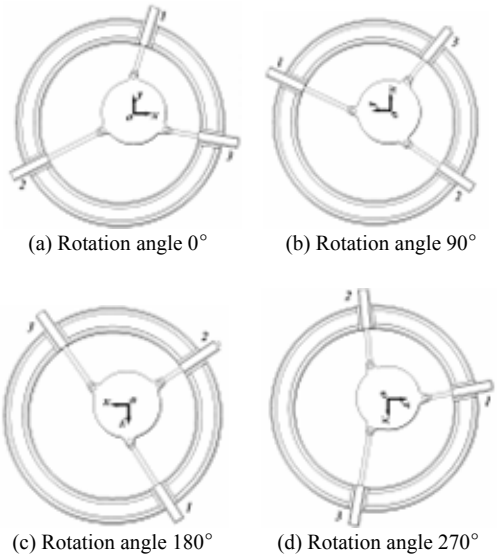

(a) Rotation angle 0° (b) Rotation angle 90°

(c) Rotation angle 180° (d) Rotation angle 270°

Fig. 2. Rotational capability of the mechanism at an arbitrary (*x, y*) position.

2. Kinematics of the mechanism

This section presents the architecture of the mechanism, followed by the procedures describing its inverse and forward kinematics. The kinematics is solved based on the Cartesian coordinate, and polar coordinates can be used to avoid coordinate coupling.

2.1 Description of the mechanism

The proposed mechanism consists of 3-PPR serial sub-chains that move independently on a fixed circular guide. Fig. 3 shows the geometric configuration of the mechanism. The mechanism has 3-DOF and three actuated joints (A_i) located along the circular guide. The connecting legs (A_iB_i) are extensible. Each extensible leg consists of two links connected by a P. The inner end of the extensible legs is mounted to the moving platform via the three Rs (B_i). The actuated Ps along the circular guide yield a continuous 360-degree rotational capability of the mechanism's platform at about the *Z*-axis in the fixed frame $\{F\}$, as shown in Fig. 3. The kinematic parameters of the mechanism are the fixed circular guide radius (r_a) and the radius of the moving platform (r_b). The actuated P values are referred to as θ_i and the P values in the connecting legs as ρ_i, where *i* stands for the index of each serial sub-chain.

2.2 Inverse kinematics

The problem of inverse kinematics is concerned with determining the values of the actuated joints from the position and orientation of the moving frame $\{M\}$, which is attached to the moving platform. The inverse kinematics of the mechanism can be solved as a whole by solving the inverse kinematics of each sub-chain. The Cartesian positions of the Rs, which are denoted as B_i in Fig. 3, are calculated from the position ($\vec{p}$) and orientation (***R***) of the moving platform in the fixed frame $\{F\}$.

$$\vec{b}_i = \boldsymbol{R}\,{}^M\vec{b}_i + \vec{p} \tag{1}$$

where ${}^M\vec{b}_i$ is the vector of the R *i* expressed in the coordinates of the moving frame. ***R*** and $\vec{p}$ are expressed in the coordinates of the fixed frame and are defined as follows:

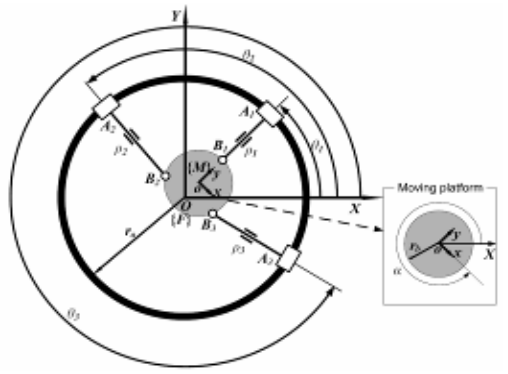

Fig. 3. Description of the mechanism and kinematic parameters.

$$\vec{p} = \begin{bmatrix} x & y \end{bmatrix}^{\mathrm{T}} \tag{2}$$

$$\boldsymbol{R} = \begin{bmatrix} \cos\alpha & -\sin\alpha \\ \sin\alpha & \cos\alpha \end{bmatrix} \tag{3}$$

where α is the angle of the moving frame with respect to the fixed frame. The actuated circular P values (A_i) are then calculated from the positions of the Rs.

$$\theta_{\mathrm{i}} = \arctan(b_{\mathrm{iy}}, b_{\mathrm{ix}}) \tag{4}$$

This can be expressed as

$$\theta_{\mathrm{i}} = \arctan\left(\frac{{}^{\mathrm{M}}\mathrm{b}_{\mathrm{ix}}\sin\alpha + {}^{\mathrm{M}}b_{iy}\cos\alpha + y}{{}^{\mathrm{M}}\mathrm{b}_{\mathrm{ix}}\cos\alpha - {}^{\mathrm{M}}\mathrm{b}_{\mathrm{iy}}\sin\alpha + x}\right) \tag{5}$$

where θ_{i} is the value of the circular P i, and b_{ix} and b_{iy} are the x and y coordinates of $\vec{b}_{\mathrm{i}}$, respectively. The Cartesian positions of the circular Ps $\vec{a}_{\mathrm{i}}$ can be determined by their joint values, and the fixed circular guide radius as follows:

$$\vec{a}_{\mathrm{i}} = \begin{bmatrix} r_{\mathrm{a}}\cos\theta_{\mathrm{i}} & r_{\mathrm{a}}\sin\theta_{\mathrm{i}} \end{bmatrix}^{\mathrm{T}}. \tag{6}$$

Eqs. (5) and (6) yield eight solutions to the inverse kinematics of this mechanism because each circular P value (θ_{i}) has two values according to the choice of the $\arctan(b_{\mathrm{iy}}, b_{\mathrm{ix}})$. The solution can be uniquely determined from the initial configuration of the mechanism and the continuity of the solution.

Additionally, by using Eqs. (1) and (6), the passive P values (ρ_{i}) in the connecting legs are determined as follows:

$$\rho_{\mathrm{i}} = \left\| \vec{a}_{\mathrm{i}} - \vec{b}_{\mathrm{i}} \right\| \tag{7}$$

2.3 Forward kinematics

The problem of forward kinematics is determining the position and orientation of the moving frame given the actuated joint values. Generally, the forward kinematics solution for most parallel mechanisms is not unique and is difficult to determine analytically. For this mechanism, the forward kinematics solution is obtained by solving the forward kinematics of each sub-chain after calculating the actuated and passive joint values. The passive joint values must be determined numerically by the actuated joint values and the kinematics constraint equation.

The kinematics constraint equation, (Eq. 8), is defined for conditions in which the distances between the Rs of the moving platform are constant and equal to, $\sqrt{3}r_{\mathrm{b}}$.

$$\vec{g}\left(\vec{\theta}_{\mathrm{a}}, \vec{\theta}_{\mathrm{p}}\right) = \begin{bmatrix} \left\| \vec{b}_1 - \vec{b}_2 \right\|^2 - 3r_{\mathrm{b}}^2 \\ \left\| \vec{b}_2 - \vec{b}_3 \right\|^2 - 3r_{\mathrm{b}}^2 \\ \left\| \vec{b}_3 - \vec{b}_1 \right\|^2 - 3r_{\mathrm{b}}^2 \end{bmatrix} = \vec{0} \tag{8}$$

where

$$\vec{b}_{\mathrm{i}} = \begin{bmatrix} (r_{\mathrm{a}} - \rho_{\mathrm{i}})\cos\theta_{\mathrm{i}} & (r_{\mathrm{a}} - \rho_{\mathrm{i}})\sin\theta_{\mathrm{i}} \end{bmatrix}^{\mathrm{T}} \tag{9}$$

$$\vec{\theta}_{\mathrm{a}} = \begin{bmatrix} \theta_1 & \theta_2 & \theta_3 \end{bmatrix}^{\mathrm{T}} \tag{10}$$

$$\vec{\theta}_{\mathrm{p}} = \begin{bmatrix} \rho_1 & \rho_2 & \rho_3 \end{bmatrix}^{\mathrm{T}} \tag{11}$$

The $\vec{\theta}_{\mathrm{p}}$ can be determined by a numerical method such as the Newton-Raphson method. The position of the moving platform ($\vec{p}$), which is the center of an equilateral triangle, and the rotation matrix can then be calculated by using $\vec{b}_{\mathrm{i}}$ as follows:

$$\vec{p} = \frac{1}{3}\left(\vec{b}_1 + \vec{b}_2 + \vec{b}_3\right), \tag{12}$$

$$\boldsymbol{R} = \begin{bmatrix} \vec{R}_{\mathrm{x}} & \vec{R}_{\mathrm{y}} \end{bmatrix}, \tag{13}$$

where

$$\vec{R}_{\mathrm{x}} = \frac{1}{\sqrt{3}r_{\mathrm{b}}}\left(\vec{b}_3 - \vec{b}_2\right) \text{ and } \vec{R}_{\mathrm{y}} = \frac{1}{r_{\mathrm{b}}}\left(\vec{b}_1 - \vec{p}\right).$$

3. Jacobian matrix

This section presents a derivation of the Jacobian matrix, which is the relationship between the velocity of the active joints, the passive joints, and the end-

effector.

3.1 Kinematic constraint Jacobian matrix

The kinematic constraint Jacobian matrix, which is a relationship between the velocity of the active joints and that of the passive joints, can be determined by differentiating Eq. (8). It can be expressed as follows:

$$\frac{\partial \vec{g}}{\partial \vec{\theta}}\dot{\vec{\theta}} = \frac{\partial \vec{g}}{\partial \vec{\theta}_{\mathrm{a}}}\dot{\vec{\theta}}_{\mathrm{a}} + \frac{\partial \vec{g}}{\partial \vec{\theta}_{\mathrm{p}}}\dot{\vec{\theta}}_{\mathrm{p}} = \vec{0} \tag{14}$$

The velocity of the passive joints can then be determined as follows:

$$\dot{\vec{\theta}}_{\mathrm{p}} = -\left(\frac{\partial \vec{g}}{\partial \vec{\theta}_{\mathrm{p}}}\right)^{-1}\frac{\partial \vec{g}}{\partial \vec{\theta}_{\mathrm{a}}}\dot{\vec{\theta}}_{\mathrm{a}}, \tag{15}$$

where the kinematic constraint Jacobian is expressed as follows:

$$\Phi = -\left(\frac{\partial \vec{g}}{\partial \vec{\theta}_{\mathrm{p}}}\right)^{-1}\frac{\partial \vec{g}}{\partial \vec{\theta}_{\mathrm{a}}}. \tag{16}$$

3.2 Forward Jacobian matrix

The forward Jacobian matrix, which is the relationship between the velocity of the active joints and that of the end-effector, can be determined by differentiating Eq. (7), which can be expressed in vector form as follows:

$$\vec{q}_i(\vec{x}, \vec{\theta}_{\mathrm{a}}, \vec{\theta}_{\mathrm{p}}) = \begin{bmatrix} \left\|\vec{a}_1 - \vec{b}_1\right\|^2 - {\rho_1}^2 \\ \left\|\vec{a}_2 - \vec{b}_2\right\|^2 - {\rho_2}^2 \\ \left\|\vec{a}_3 - \vec{b}_3\right\|^2 - {\rho_3}^2 \end{bmatrix} = \vec{0} \tag{17}$$

where

$$\vec{x} = \begin{bmatrix} x & y & \alpha \end{bmatrix}^{\mathrm{T}}.$$

The resulting differentiated Eq. can then be expressed as follows:

$$\frac{\partial \vec{q}}{\partial \vec{x}}\dot{\vec{x}} + \frac{\partial \vec{q}}{\partial \vec{\theta}_{\mathrm{a}}}\dot{\vec{\theta}}_{\mathrm{a}} + \frac{\partial \vec{q}}{\partial \vec{\theta}_{\mathrm{p}}}\dot{\vec{\theta}}_{\mathrm{p}} = \vec{0}. \tag{18}$$

The velocity of the end-effector can then be determined by solving

$$\dot{\vec{x}} = -\left(\frac{\partial \vec{q}}{\partial \vec{x}}\right)^{-1}\left(\left(\frac{\partial \vec{q}}{\partial \vec{\theta}_{\mathrm{a}}}\right) + \frac{\partial \vec{q}}{\partial \vec{\theta}_{\mathrm{p}}}\Phi\right)\dot{\vec{\theta}}_{\mathrm{a}}, \tag{19}$$

where the forward Jacobian is expressed as

$$J_f = -\left(\frac{\partial \vec{q}}{\partial \vec{x}}\right)^{-1}\left(\left(\frac{\partial \vec{q}}{\partial \vec{\theta}_{\mathrm{a}}}\right) + \frac{\partial \vec{q}}{\partial \vec{\theta}_{\mathrm{p}}}\Phi\right). \tag{20}$$

4. Singularity analysis

A singularity is a configuration in which the number of DOF in the mechanism increases or decreases instantaneously. Singularities are one of the most significant and critical problems in the design and control of parallel mechanisms because they lead to loss of controllability, breakage, and degradation of stiffness in the mechanism.

Singularities can be classified into three types: configuration space, actuator, and end-effector [14]. A configuration space singularity is the intersection of all possible actuator singularities. Actuator singularities are configurations in which some links in the mechanism can move when the actuators are locked, or in which actuator forces cause the mechanism to break down. End-effector singularities are configurations in which the end-effector of the mechanism instantaneously loses mobility in one or more DOF. The three kinds of singularities occur in the following conditions, respectively:

$$rank\left(\frac{\partial \vec{g}}{\partial \vec{\theta}}\left(\theta_{\mathrm{j}}\right)\right) < 3 \tag{21}$$

$$rank\left(\frac{\partial \vec{g}}{\partial \vec{\theta}_{\mathrm{p}}}\left(\theta_{\mathrm{j}}\right)\right) < 3 \tag{22}$$

$$rank\left(J_f\left(\theta_{\mathrm{j}}\right)\right) < 3 \tag{23}$$

where

$$\vec{\theta} = \begin{bmatrix} \vec{\theta}_{\mathrm{a}} & \vec{\theta}_{\mathrm{p}} \end{bmatrix}^{\mathrm{T}}.$$

To determine the singular configuration, the condition number, which is defined as the ratio of the maximum singular value to the minimum singular value, is computed in the workspace. As the matrices in Eqs. (21)-(23) are nonlinear simultaneous equations, the numerical method using the condition number is more suitable than calculating the analytical solution of the equations. In the analysis, the singular-

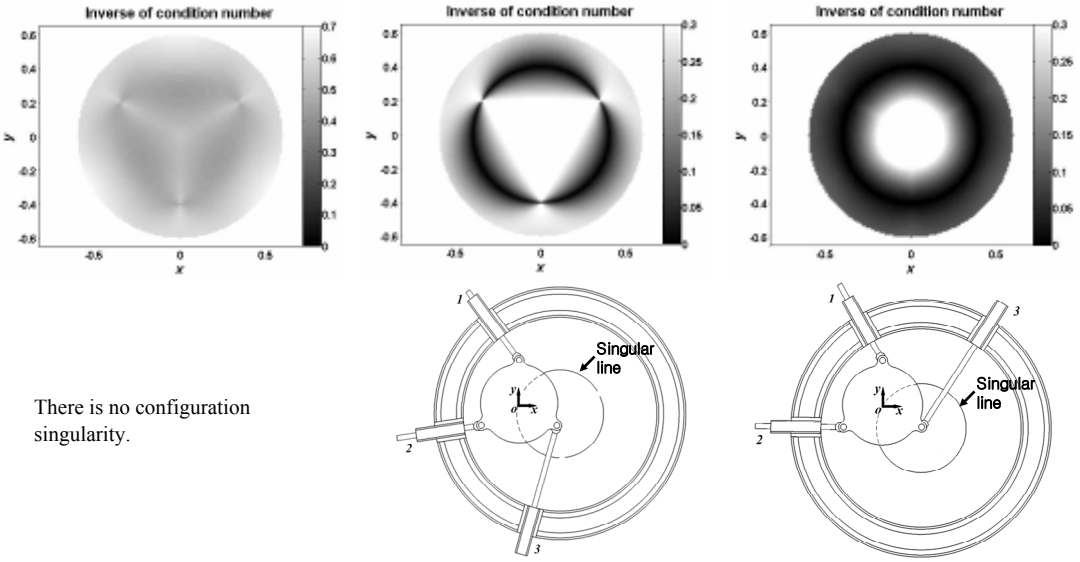

(a) Configuration singularity (b) Actuator singularity (c) End-effector singularity

Fig. 4. Singularity analysis using the inverse of the condition number and an example of a singular configuration.

ity occurs when the inverse of the condition number equals zero. For calculation, r_b is assumed equal to $0.4r_a$ For all rotation angles of the moving platform, the same singular configurations exist in this mechanism. Accordingly, the rotation angle of the moving platform is specified as 0 degree.

The upper part of Fig. 4 shows the inverse of the condition number in the reachable workspace, and the bottom part shows the example of each singular configuration. In the entire workspace, there is no configuration space singularity, and the other two types of singularities (actuator and end-effector) coexist in the workspace. The actuator and end-effector singularities occur when the moving platform is located on the boundary of the circle with a radius of r_b and at the center of the fixed frame, which is shown in Figs. 4 (b) and (c). This excludes cases in which one of the moving platform's Rs is also located at the center.

5. Workspace analysis

The workspace of a mechanism refers to the full set of positions and orientations achievable by the moving frame. It is determined by the mechanism's architecture and the angular and translational displacement capabilities of each link. For parallel mechanisms, the workspace is limited by the need to avoid collision between the mechanical parts and the limits of the displacement in the joints. A detailed workspace analysis is the most important step in the design of parallel mechanisms, and it has thus received attention from several researchers [9, 15].

The workspace analysis of the mechanism proposed here has been conducted by checking for the intersection of positions of the moving frame for all possible rotation angles. Considering the mechanism's kinematic constraints that the moving platform always exists in the fixed circular guide and that there is no interference between the circular Ps, the workspace is circular with a radius of r_a-r_b. This workspace is dexterous, which is defined to be the set of points that can be reached with any arbitrary orientation of the moving frame.

However, as discussed in Section 4, two types of singularities occur in the workspace, which is determined by the kinematic constraints when the radius of the moving platform (r_b) is less than or equal to $0.5r_a$. These singularities lead to serious problems in the mechanism, such as breakage and loss of controllability. Thus, the singularity-free workspace must be selected and maximized for practical applications. This singularity-free workspace is circular and has a radius of r_s, which depends on r_b. The relationship between r_s and r_b is expressed as follows:

$$r_s = \begin{cases} r_b & (r_b \le 0.5r_a) \\ r_a - r_b & (r_b > 0.5r_a) \end{cases} \tag{24}$$

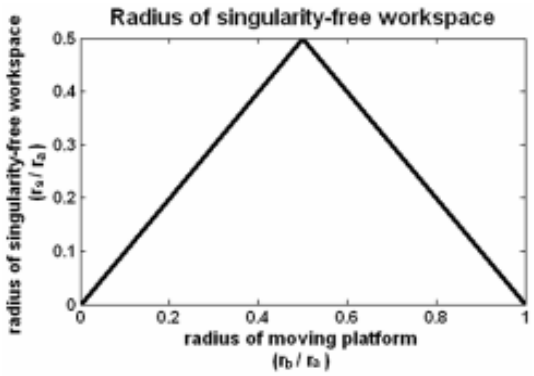

Fig. 5. Radius of the singularity-free workspace along the radius of moving platform (r_b/r_a).

Fig. 5 shows the radius of the singularity-free workspace (r_s) with respect to r_b, illustrating that the singularity-free workspace is maximized when the r_b is equal to 0.5 r_a.

6. Application example of the platform: PCB depaneling machine

To separate the individual PCB from the bigger production panel, the PCB depaneling system consists of a feeder, a positioning device, and a bridge-cutting tool. Generally, the *X*-*Y* stage and the milling cutter are used as the positioning device and cutting tool, respectively. However, there are three major drawbacks: heavy moving mass, excessive milling dust, and danger of the tool breaking.

Fig. 6 shows the suggested conceptual design of the PCB depaneling system. A punching tool is adopted as the cutting tool of a bridge, as the punching process can reduce the cutting time and the volume of milling dust. The working life of the tool can also be extended. The punching tool has drawbacks in that the die needs to cut the bridge, and the orientation of the punch should be aligned along with the bridge.

The proposed 3-DOF planar parallel mechanism is used as the positioning device of the PCB. As the parallel mechanism has an open space above and below the end-effector, the synchronized punch-die can be operated effectively. In addition, because the orientation of the punching tool is fixed, the high rotation capability can carry out bridge cutting in an arbitrary orientation. The proposed PCB depaneling system using the punching tool and parallel mechanism has the advantages of small moving mass, no milling dust, and long tool life.

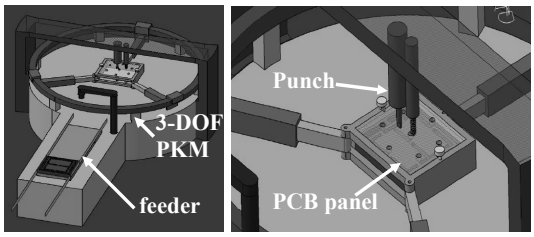

(a) Proposed PCB (b) Enlarged punching tool part depaneling system

Fig. 6. Conceptual design of the PCB depaneling machine using the planar parallel mechanism and a punching tool.

7. Conclusion

This paper has presented a new planar parallel mechanism with one rotational and two translational DOF capable of a continuous 360-degree rotation of the platform. The kinematics, singularities, and workspace aspects have been analyzed to validate the reliability of the proposed mechanism as a positioning platform. The mechanism has been proven to have a 360-degree rotation in the 0.5r_a radius of a circle-shaped singularity-free workspace. One applicable example for the PCB depaneling machine has also been proposed. The mechanism can be used in various fields where high rotational capability is required.

Acknowledgment

This work is supported by the Brain Korea 21 Project, SNU-IAMD, and partly by Engineering Research Center for Micro-thermal Systems.

References

[1] J.-P. Merlet, *Parallel Robots*, Kluwer Academic Publishers, Dordrecht, Boston, London, (2000).

[2] D. Stewart, A platform with six degrees of freedom, *Proc. Inst. Mech. Eng.*, 1 (15) (1966) 371-386.

[3] J. Kim, F. C. Park, S. J. Ryu, J. Kim, J. Hwang, C. Park and C. Iurascu, Design and analysis of a redundantly actuated parallel mechanism for rapid machining, *IEEE Transactions on Robotics and Automation*, 17 (4) (2001) 423-434.

[4] J. Kim, J-C. Hwang, J-S. Kim, C. Iurascu, F. C. Park and Y. M. Cho, Eclipse-II: A new parallel mechanism enabling continuous 360-degree spinning plus three-axis translational motions, *IEEE Transactions on Robotics and Automation*, 18 (3) (2002) 367-373.

[5] A. H. Shirkhodetie and A. H. Soni, Forward and inverse synthesis for a robot with three degrees of freedom, *Proc. of the Summer Computer Simulation Conference,* MontrCal, (1987) 851-856.

[6] C. M. Gosselin, S. Lemieuxt and J. -P. Merlet, A new architecture of planar three-degree-of-freedom parallel Manipulator, *Proc. of IEEE International Conference on Robotics and Automation*, Minneapolis, Minnesota (1996).

[7] X.-J. Liu, Q.-M. Wang and J. Wang, Kinematics, dynamics and dimensional synthesis of a novel 2-DoF translational manipulator, *Journal of Intelligent and Robotic Systems*, 41 (4) (2005) 205-224.

[8] H. Li, C. M. Gosselin and M. J. Richard, Determination of maximal singularity-free zones in the workspace of planar three-degree-of-freedom parallel mechanisms, *Mechanism and machine theory*, 41 (10) (2006) 1157-1167.

[9] J.-P. Merlet, C. M. Gosselin and N. Mouly, Workspaces of planar parallel manipulators, *Mechanism and Machine Theory*, 33 (1) (1998) 7-20.

[10] K.-B. Choi, Kinematic analysis and optimal design of 3-PPR planar parallel manipulator, *KSME International Journal*, 17 (4) (2003) 528-537.

[11] Y.-J. Nam and M.-K. Park, Kinematics and optimization of 2-DOF parallel manipulator with revolute actuators and a passive leg, *Journal of Mechanical Science and Technology*, 20 (6) (2006) 828-839.

[12] W. In, S. Lee, J. I. Jeong and J. Kim, Design of a planar-type high speed parallel mechanism positioning platform with the capability of 180 degrees orientation, *CIRP Annals - Manufacturing Technology*, 57 (1) (2008) 421-424.

[13] D. S. Kang, T. W. Seo and J. Kim, Development and kinematic calibration for measurement structure of a micro parallel mechanism platform, *Journal of Mechanical Science and Technology*, 22 (4) (2008) 746-754.

[14] F. C. Park and J. W. Kim, Singularity analysis of closed kinematic chains, *ASME J. Mechanical Design*, 121 (1) (1998) 32-38.

[15] F. Gao, X.-J. Liu and X. Chen, The relationships between the shapes of the workspaces and the link lengths of 3-DOF symmetrical planar parallel manipulators, *Mechanism and Machine Theory*, 36 (2) (2001) 205-220.

Tae Won Seo received the B. S. and Ph. D. degree in the school of mechanical and aerospace engineering from Seoul National University (SNU), Seoul, Korea, in 2003 and 2008. He was with BK21 school of creative design of next generation mechanical and aero-space systems in SNU as a post-doctoral researcher from 2008 to 2009, and in the same period, he was also with institute of advanced machinery and design in SNU as a post-doctoral researcher. He is currently a post-doctoral research associate of Nanorobotics laboratory in department of mechanical engineering, Carnegie-Mellon University. His current research interests include mechanism design, optimal design, control, and motion planning of robotic systems.

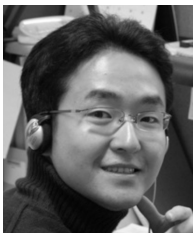

Woosung In received his Ph.D. from the School of Mechanical and Aerospace Engineering of the Seoul National University in 2008. Currently, he is with digital media team, Samsung Electronics, Korea. His research interests are synthesis and analysis of a parallel mechanism, redundant actuation of a parallel mechanism, and Biomechanics.

Jongwon Kim is a professor at the School of Mechanical and Aerospace Engineering of Seoul National University, Korea. He received his BS in Mechanical Engineering from the Seoul National University in 1978 and his MS in Mechanical and Aerospace Engineering from KAIST, Korea, in 1980. He received his Ph.D. in Mechanical Engineering from the University of Wisconsin-Madison, USA, in 1987. He worked for Daewoo Heavy Industry & Machinery, Korea, from 1980 to 1984. From 1987 to 1989, he was the Director of the Central R&D Division of Daewoo Heavy Industry & Machinery. From 1989 to 1993, he was a researcher at the Automation and Systems Research Institute of the Seoul National University. His research interests include parallel mechanism, Taguchi methodology, and field robots.